

# Journal of Materials Chemistry A

Accepted Manuscript



This is an *Accepted Manuscript*, which has been through the Royal Society of Chemistry peer review process and has been accepted for publication.

*Accepted Manuscripts* are published online shortly after acceptance, before technical editing, formatting and proof reading. Using this free service, authors can make their results available to the community, in citable form, before we publish the edited article. We will replace this *Accepted Manuscript* with the edited and formatted *Advance Article* as soon as it is available.

You can find more information about *Accepted Manuscripts* in the [Information for Authors](#).

Please note that technical editing may introduce minor changes to the text and/or graphics, which may alter content. The journal's standard [Terms & Conditions](#) and the [Ethical guidelines](#) still apply. In no event shall the Royal Society of Chemistry be held responsible for any errors or omissions in this *Accepted Manuscript* or any consequences arising from the use of any information it contains.

Cite this: DOI: 10.1039/x0xx00000x

Received 00th January 2012,  
Accepted 00th January 2012

DOI: 10.1039/x0xx00000x

www.rsc.org/

## Lasting and Self-Healing Superhydrophobic Surfaces by Coating of Polystyrene/SiO<sub>2</sub> Nanoparticles and Polydimethylsiloxane

Chao-Hua Xue<sup>\*a,b</sup>, Zhi-Dong Zhang<sup>a</sup>, Jing Zhang<sup>a</sup>, and Shun-Tian Jia<sup>a</sup>

Maintaining hierarchical roughness and low surface-energy property are keys to long lasting superhydrophobic surfaces. By spraying polystyrene/SiO<sub>2</sub> core/shell nanoparticles as a coating skeleton and polydimethylsiloxane as hydrophobic interconnection, lasting and self-healing superhydrophobic surfaces were fabricated. The coating could expose new roughening structures during the rubbing process, thus maintaining suitable hierarchical roughness, favouring superhydrophobic property of the surface. Also, the superhydrophobicity of damaged surface from air plasma treatment could be restored automatically in 12 h at room temperature, or by heat curing and tetrahydrofuran treatment, which helped with the release of hydrophobic polystyrene. This strategy might find practical applications in all kinds of substrates since spray coating is a simple process and the obtained surfaces possess lasting superhydrophobicity.

### Introduction

Superhydrophobic surfaces with water contact angles greater than 150° and slide angles lower than 10° have received great interest within the scientific community as well as the industrial world over the last two decades.<sup>1-9</sup> Most importantly, much attention has been paid to prolonging the lifespan of superhydrophobic surfaces in recent years,<sup>1, 2, 5, 10-12</sup> which is significant for the employment of the materials in practical applications. One approach to increase the life time of superhydrophobic materials is to use mechanically durable hydrophobic materials.<sup>13-16</sup> For example, Su et al.<sup>17</sup> fabricated durable superhydrophobic coatings using polyurethane with polydimethylsiloxane (PDMS) side chains. The materials demonstrated resistance to 10 000 rubbings at loads of 2945.7 Pa at 18 cm s<sup>-1</sup>. Zhou et al.<sup>3</sup> used PDMS, filled with fluorinated alkyl silane (FAS) functionalised silica nanoparticles and FAS, to produce a superhydrophobic coating on fabrics. This coating showed remarkable durability against strong acid, strong alkali, repeated machine washes, boiling water, and severe abrasion, whilst retaining its superhydrophobicity. Xue et al.<sup>2</sup> fabricated lasting superhydrophobic and colorful surfaces through chemical etching of poly(ethylene terephthalate) fiber surfaces, followed by diffusion of fluoroalkylsilane into fibers. The obtained superhydrophobic textiles showed strong durability against severe abrasion, long-time laundering, and boiling water.

Another approach to improve durability of superhydrophobic surfaces is to endow materials with the ability to regenerate the surface roughness or/and restore the hydrophobic components. The key to superhydrophobic surfaces lies with the combination of surface chemical compositions and topographic structures.<sup>1</sup> Wearing occurs very often for materials used in everyday life. When part of the material is damaged, exposing new roughening hydrophobic structures on the newly formed surface is possible to avoid losing superhydrophobic properties. Deng et al.<sup>18, 19</sup> reported transparent and robust superamphiphobic surfaces by coating a porous deposit of candle soot with a 25 nanometer thick silica shell, followed by calcination at 600 °C and silanization. The coating remained superamphiphobic even after its top layer was damaged by sand impingement. It was found that the sand-abraded area revealed almost unaltered submicrometer morphology. Due to the coating's self-similarity, the surface kept its superamphiphobicity until the layer was removed after extended impact. The wear regeneration of surface patterns was also demonstrated by Jin et al.<sup>20</sup>

Besides wearing, restoration of hydrophobic components at surfaces through self-healing to preserve superhydrophobicity has also attracted great interest.<sup>14, 21-26</sup> Li et al.<sup>10, 27</sup> fabricated superhydrophobic coatings with preserved self-healing agents of reacted fluoroalkylsilane (FAS) in the coatings, which were porous and rigidly flexible. Once the primary top FAS layer was decomposed, rendering the surface hydrophilic, the preserved healing agents could migrate to the coating surface in a humid environment to heal the superhydrophobicity of the coating. Wang et al.<sup>28, 29</sup> demonstrated that fabrics coated with a hydrolysis product from fluorinated-decyl polyhedral oligomeric silsesquioxane (FD-POSS) and a fluorinated alkyl silane had a remarkable self-healing functionality of superhydrophobicity. When polar groups appeared after chemical damage of the surface that resulted in reduced surface

*a* College of Resource and Environment, Shaanxi University of Science and Technology, Xi'an 710021, China.

*b* Shaanxi Research Institute of Agricultural Products Processing Technology, Shaanxi University of Science and Technology, Xi'an 710021, China. E-mail: xuech@zju.edu.cn

† Electronic supplementary information (ESI) available.

hydrophobicity, heating the coating layer could increase the mobility of the FD-POSS molecules. As a result of molecular rotation and movement, the introduced polar groups tended to be hidden inside the coating layer and more fluorinated alkyl chains became exposed to the surface, healing the superhydrophobicity. Other works using perfluorooctyl acid<sup>22</sup> contained in alumina nanopores and octadecylamine<sup>23</sup> encapsulated in mesoporous silica as healing agents for self-healing superhydrophobic surfaces were also reported.

Making hydrophobic materials that can maintain roughened structures or/and fabricating roughened surfaces that can maintain low surface-energy properties during applications provide an effective way to obtain long lasting superhydrophobicity.<sup>10, 24</sup> Herein, we report the fabrication of lasting and self-healing superhydrophobic surfaces by spraying polystyrene/SiO<sub>2</sub> core/shell nanoparticles as a coating skeleton with polydimethylsiloxane as hydrophobic interconnection. The coating could expose new roughening structures during the rubbing process, thus maintaining suitable hierarchical roughness, favouring superhydrophobic property of the surface. Also, the superhydrophobicity of damaged surface from air plasma treatment could be restored automatically in 12 h at room temperature, or by heat curing and tetrahydrofuran treatment.

## Experimental section

### Materials

Styrene was purchased from Tianli Chemical Reagent Co., Ltd. Tetraethoxysilane (TEOS) and polyvinylpyrrolidone (PVP) were purchased from Tianjin Kemiou Chemical Reagent Co., Ltd. 2,2'-Azobis (2-methylpropionamide) dihydrochloride (AIBA) was purchased from Qingdao Kexin New Materials Science and Technology Co., Ltd. Polydimethylsiloxane (PDMS, Sylgard 184 Silicone Elastomer Kit with components of PDMS base and curing agent) was purchased from DOW CORNING. Diglycidyl ether of bisphenol A (DGEBA, trade name as E-44) was purchased from FeiCheng DeYuan Chemicals Co., Ltd. Polyimide resin was purchased from ZhongDe Chemicals Co., Ltd. Tetrahydrofuran (THF), hexane, ethanol (EtOH), hydrochloric acid (HCl), distilled water, acetone, and glass slides were obtained commercially. All chemicals were used as received.

### Preparation of polystyrene /SiO<sub>2</sub> core/shell nanoparticles

To a three-necked flask, 3 g of styrene, 1 g of PVP, and 90 mL of water were added, and the mixture was vigorously stirred at 120 rpm for about 10 min at room temperature. Then, 0.4 g of AIBA dissolved in 10 mL of water was added to the mixture. After this, the reaction solution was deoxygenated under a nitrogen atmosphere at room temperature for 1 h and heated to 75 °C for 24 h under a constant stirring rate of 120 rpm to obtain the PS colloid.

To fabricate PS/SiO<sub>2</sub> core/shell particles, the pH of the obtained PS colloid was adjusted to 4.0 using HCl solution. Then, 1.5 g of TEOS was added drop wise to 30 g of PS colloid. The hydrolysis and condensation reaction of TEOS was carried out under constant stirring at 40 °C for 24 h, directly yielding PS/SiO<sub>2</sub> core/shell structural spheres. The core-shell particles were centrifuged and washed with copious water and ethanol twice, and then diluted in ethanol to form a PS/SiO<sub>2</sub> dispersion. Before use, the suspension was sonicated for a few minutes to disperse the core/shell particles.

### Fabrication of superhydrophobic surfaces

Glass slides were cleaned successively by acetone, deionized water, and ethanol under ultrasonic condition, and dried for use. A base-coat solution of epoxy resin was prepared by dissolving 0.15 g of DGEBA and 0.1 g of polyimide resin into 30 g of THF. A PDMS solution was prepared by dissolving 1 g of PDMS and 0.2 g of curing agent into 19 g of hexane solution.

Glass substrates were first spray-coated with epoxy resin base-coat solution, and cured at 80 °C for 10 min. Then the epoxy coated substrates were spray-coated with the PS/SiO<sub>2</sub> ethanol dispersion (0.7 wt %) and dried at room temperature. Under these conditions, the alcohol solvent volatilized rapidly, leading to deposition of the PS/SiO<sub>2</sub> particles onto the substrates. This spray coating was repeated 15 times (5, 10, and 20 coatings were also done) before the substrates were cured at 150 °C for 1 h. Finally, the PS/SiO<sub>2</sub> coated substrates were spray-coated with PDMS solution for 10 s, and cured at 150 °C for 1 h to obtain stable superhydrophobic surfaces. The final coatings that were sprayed with core-shell particles 5, 10, 15 and 20 times were named S-5, S-10, S-15, and S-20, respectively.

### Characterization

The morphology of PS and PS/SiO<sub>2</sub> particles was characterized by TEM and SEM. TEM analysis was performed by using a transmission electron microscope (Hitachi H600) operated at an accelerating voltage of 100 kV. Samples for TEM analysis were prepared at room temperature by placing one droplet of ethanol dispersion of the sample on a copper grid, and then letting it dry. SEM analysis was performed by using a field emission scanning electron microscope (Hitachi, FE-SEM S4800). Samples for SEM analysis were prepared by placing 0.1 μL of ethanol dispersion of the sample on an aluminum sheet, letting it dry and then sputter-coating it with gold. The surface morphology of the as-obtained superhydrophobic surfaces was also observed by SEM. XPS measurements were carried out on a Thermo Scientific K-Alpha XPS spectrometer. The topography of the superhydrophobic surfaces and the abrasive coatings was observed using atomic force microscopy (Multi Mode, NanoScope IIIa) operated in contact mode. The root-mean-square (RMS) roughness values were calculated from 10 μm×10 μm images.

The static contact angle (CA) of water on the surfaces was measured with a Contact Angle Meter (OCA 20, Dataphysics, Germany). A droplet of water (5 μL) was placed onto the film. The CA was measured on five different sites for each sample. The mean value was taken as the final result. Double-distilled water with a measured surface tension of 72 mN·m<sup>-1</sup> was used in this analysis. The sliding angle was also measured. Advancing and receding CAs were recorded during adding/withdrawing water at a rate of 0.1 μL/s introduced by built-in syringe pump. The contact angle hysteresis (CAH) was calculated by taking the difference between advancing and receding CA.

The abrasion resistance of the coating was evaluated by sand impact. The sample was abraded different times by impinging the coating surface with fifty grams of 300 to 1000 μm diameter sand grains from a height of 40 cm at 45 ° (Fig. S1).

The healing ability of the superhydrophobic surfaces was evaluated by air plasma etching of the substrates. Air plasma etchings were carried out using a YZD08-5C plasma cleaner (Tangshan Yanzhao Science and Technology Institute, China) at high vacuum under a power of 40 W for 5 min. For healing of the surfaces at ambient temperature, the etched coatings were kept at room temperature and the CA was tested every 3 h. For healing by heat treatment, the etched coatings were cured at 150 °C for 1 h. For healing by THF treatment, the etched coatings were sprayed with THF solution for over 4 s and then cured at 150 °C for 1 h.

## Results and discussion

### Morphology of PS@SiO<sub>2</sub> spheres

SEM and TEM images of the PS and PS/SiO<sub>2</sub> samples are shown in Fig. 1. The as-prepared PS sample showed perfectly monodisperse smooth spheres with an average diameter of about 157 nm, as shown in Fig. 1(a) and (b).

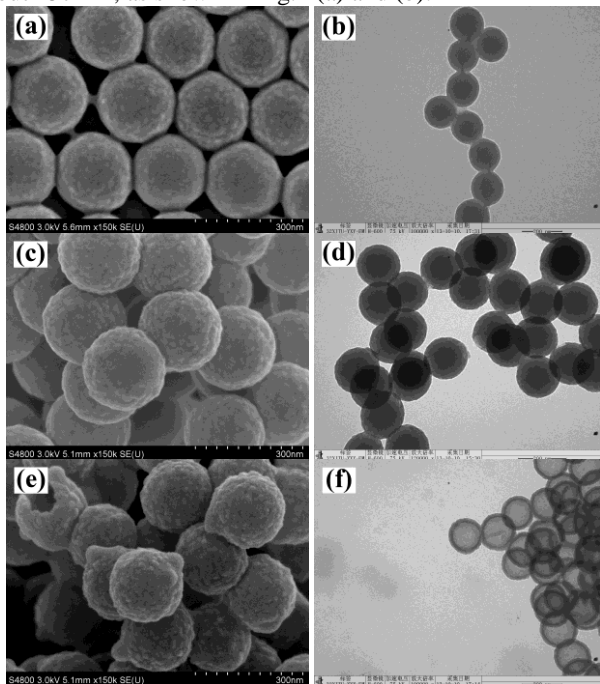


**Fig. 1** SEM images of (a) PS, (c) PS/SiO<sub>2</sub>, and (e) THF treated PS/SiO<sub>2</sub>; TEM images of (b) PS, (d) PS/SiO<sub>2</sub>, and (f) THF treated PS/SiO<sub>2</sub>

After coating with silica by hydrolysis of TEOS under acid condition, the spheres showed a particle-decorated surface with a small increase in diameter (Fig. 1c). It seemed difficult to determine whether core/shell structures were formed from the TEM image of Fig. 1(d). However, after treatment with THF, broken hollow spheres were found in the SEM image of Fig. 1(e) and smooth spherical hollow shells were found in the TEM image of Fig. 1(f). These results provided evidence of the core/shell structure of PS/SiO<sub>2</sub> nanoparticles before removal of the PS core by THF.

The removal of PS core from PS/SiO<sub>2</sub> indicated that, under certain conditions, the inner PS could migrate through the silica shell, which is usually mesoporous<sup>30, 31</sup>. This migration of PS from PS/SiO<sub>2</sub> particles might provide a way to reduce the surface energy of the silica-based coating, since PS was a hydrophobic polymer that was often used to prepare superhydrophobic coatings<sup>32-34</sup>. It is known that silica particles are hydrophilic. However, spraying THF solution on the PS/SiO<sub>2</sub> coated substrate without PDMS for 10 s, followed by curing in 150 °C for 1h made the surface superhydrophobic, as shown in the inset of Fig. 2. THF treatment and curing obviously drove the PS to migrate from the core to the surface, forming a coating on silica and some connections between particles. This is shown in Fig. 2, where some hollow silica

particles were also found due to the THF swelling<sup>35</sup> and PS removal. In combination with the particulate roughening effect, the initially hydrophilic surface became superhydrophobic with a contact angle of 155.9 °.

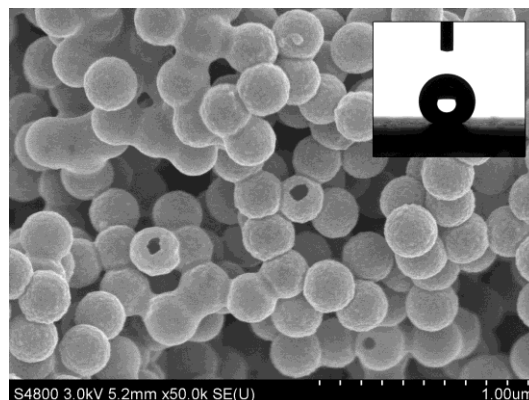
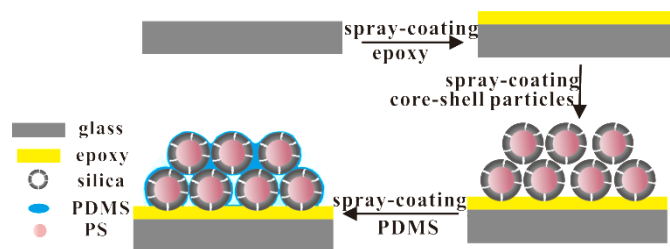


**Fig. 2** CA and SEM of PS/SiO<sub>2</sub> surface without PDMS coating after THF treatment

### Wettability and stability of PS/SiO<sub>2</sub> surfaces coated with PDMS

From Fig. 1 and Fig. 2, there are large spaces between PS/SiO<sub>2</sub> particles, resulting in a roughened surface and favouring the formation of a superhydrophobic coating after a decrease in the surface energy. However, the coating might be fragile due to the weak interactions between particles. To obtain strong coatings, the substrates were first coated with epoxy resin before PS/SiO<sub>2</sub> spraying to strengthen the interaction between particles and the substrates, and then sprayed with PDMS solution. The PDMS penetrated into the spaces between particles and acted as interconnections between particles. It also covered the PS/SiO<sub>2</sub> coating, lowering its surface energy. The fabrication process is illustrated in Scheme 1. The PS/SiO<sub>2</sub> coating became superhydrophobic after coating with PDMS. It had a contact angle of 167.2 °, taking S-15 as an example as shown in Fig. 3(a). Also, water drops moved easily on its surface, with a sliding angle of 2 °, as shown in Fig. 3(b).



**Scheme 1** Fabrication of superhydrophobic surface by coating of polystyrene/SiO<sub>2</sub> nanoparticles and polydimethylsiloxane

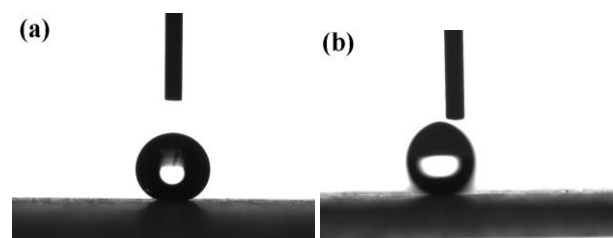


**Fig. 3** CA (a) and SA (b) of original robust coating of S-15

In order to investigate the influence of spray-coating times on the lasting and self-healing capability of coatings, sand abrasion tests were conducted on the all samples. CAs and CAHs of samples before and after different sand impact times are shown in Fig. 4. It was found that an increase in sand abrasion times resulted in a gradual reduction in the CAs, and an increase in the CAHs. After 5 abrasion impact times, S-5 had CA of  $149.6^\circ$  and CAH of  $15.4^\circ$ , and S-10 had CA of  $149.1^\circ$  and CAH of  $28.6^\circ$ , while the CAs of S-15 and S-20 were both above  $160^\circ$  and CAHs were lower than  $10^\circ$ . After 10 abrasion impact times, S-20 had CA of  $150.9^\circ$  and CAH of  $20.6^\circ$ , but S-15 was still above  $160^\circ$  and lower than  $10^\circ$ . After 20 abrasion impact times, S-15 had CA of  $158.1^\circ$  and CAH of  $22.5^\circ$ , and this surface was a sticky one but still superhydrophobic, while others turned to hydrophobic with CA much lower than  $150^\circ$ . This indicates that fewer or more spray times than 15 are not favourable to superhydrophobicity of the coating.

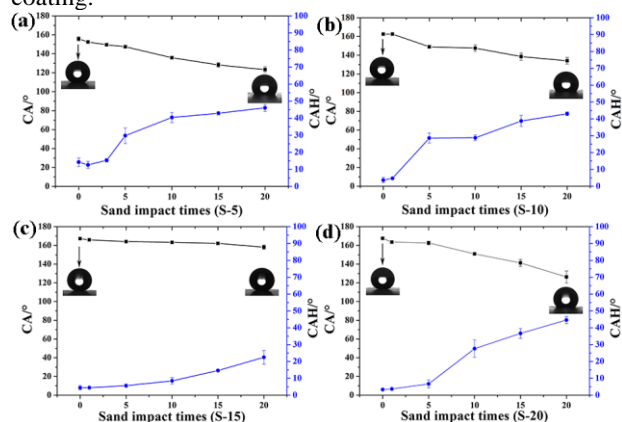


**Fig. 4** CA and CAH of coatings after different sand impact times: (a) S-5, (b) S-10, (c) S-15 and (d) S-20.

Coatings with different spray times might show different capability of retaining surface roughness after sand abrasion. SEM images of the sand impacted superhydrophobic PS/SiO<sub>2</sub> surface (S-15) are shown in Fig. 5. The surfaces were still rough after many sand abrasion impact times and the coating had a porous network structure that contained self-similar SiO<sub>2</sub> networks covered with PDMS. After several sand abrasion impact times, the surfaces still displayed silica particles coated with PDMS. An increase in abrasion impact times resulted in the coatings becoming smoother. However higher magnification showed that the surfaces were still rough. It seemed that PDMS could protect silica and provide low surface energy. Also, this surface could retain its superhydrophobicity after many sand impact times. After 20 impact times, the epoxy resin layer nearly became exposed, showing sticking superhydrophobic property with a CA of  $158.1^\circ$ . AFM 3D topography images<sup>36</sup> are shown in Fig. S2. The surface topography indicated by the AFM images agreed very well with that from the SEM images. An increase in sand abrasion times resulted in a gradual reduction in roughness of the coatings (shown in Table 1), which led to the decrease of superhydrophobicity.

**Table 1** The mean roughness of sand impact coatings (S-15)

Samples	RMS (nm)
Superhydrophobic surface (S-15)	365.08
Impact 1 time	316.99
Impact 10 times	285.42
Impact 20 times	162.37

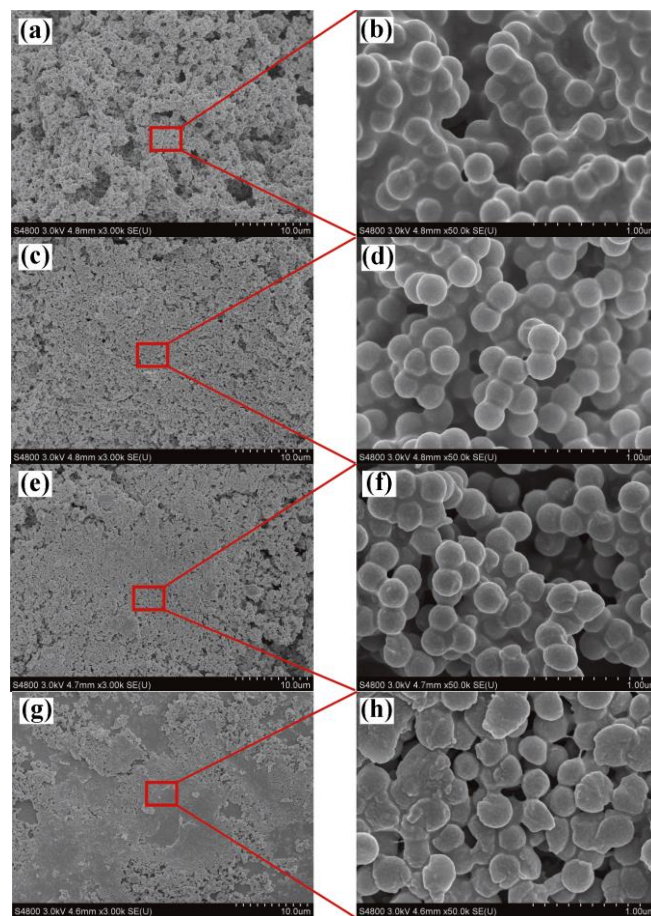


**Fig. 5** SEM images of superhydrophobic S-15 surfaces: (a) original; (b) higher magnification of (a); (c) impacted 1 time; (d) higher magnification of (c); (e) impacted 10 times; (f) higher magnification of (e); (g) impacted 20 times; (h) higher magnification of (g).

Coatings with fewer spray times, such as 5 or 10, got easily smooth after 3/10 times sand abrasion, resulting in loss of superhydrophobicity. This could be approved by the morphology changes of the coatings (Fig. S3a-h). As for the coating of S-20, the SEM image with higher magnification of the sample after 10 abrasion times showed collapsed particles (Fig. S3i-l), which were different from the morphologies of other samples. This might be because that higher spray times caused much porous outmost coating (Fig. S3i-j) due to the leaking of PDMS with solvent into the bottom. Therefore, the obtained outmost surface collapsed easily to become a smooth one (Fig. 3k-l), resulting in loss of superhydrophobicity.

### Self-healing of superhydrophobic PS/SiO<sub>2</sub> surfaces

The self-healing ability of the superhydrophobic PS/SiO<sub>2</sub> coatings was investigated by treating the film with air plasma and leaving the etched coatings in atmosphere at room temperature. It was found that air plasma treatment under a power of 40 W for 5 min turned the superhydrophobic coatings into superhydrophilic ones, which could be wetted instantly by contacting with a drop of water. This superhydrophilic transformation might be caused by the decomposition of the PDMS on its surface and the introduction of polar groups<sup>28</sup>. However, after exposure in an ambient environment for 12 h, the original superhydrophobicity of the etched coating was restored (S-15 in Fig. 6), indicating that the surface of the

damaged superhydrophobic coating was covered again with the hydrophobic PDMS. Also, an increase in the etching cycles led to an increase in the time needed to recover the superhydrophobicity of the surfaces, indicating that the healing became more difficult. This might be due to the rotation and movement of PDMS polymer chains that are thermodynamically driven by minimizing the surface tension. As a result, the introduced polar groups tended to be hidden inside the coating layer, and more PDMS chains were exposed to the surface, minimizing the surface free energy. SEM images in Fig. 7(a) showed that the etching-healing processes did not change the morphology of the coatings.

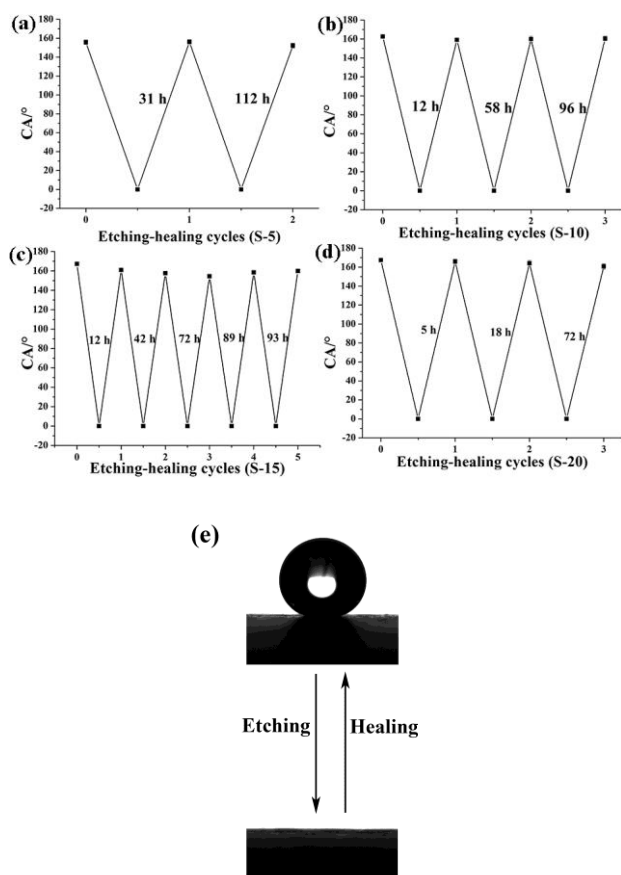


**Fig. 6** Self-healing cycles of coatings automatically healed at ambient temperature: (a) S-5, (b) S-10, (c) S-15 and (d) S-20. (e) Reversible transition between superhydrophobic and superhydrophilic state.

The first self-healing time became shorter with an increase in the spray time. From Fig. 6, it can be seen that S-20, S-10, and S-5 samples required 5 h, 12 h, and 31 h to self-heal, respectively. For the second time self-healing, it needed longer time to self-heal, also indicating that the healing became more difficult. And the S-15 samples had longer etching-healing cycles, which showed best self-healing property at ambient temperature in reasonable time. As for coatings with fewer spray times, larger amount of PDMS covered the particles and formed cured compact PDMS film on the surface, thus the reversible transitions between superhydrophobic and superhydrophilic state as shown in Fig. 6(e) might be difficult due to the limited rotation of PDMS chains.

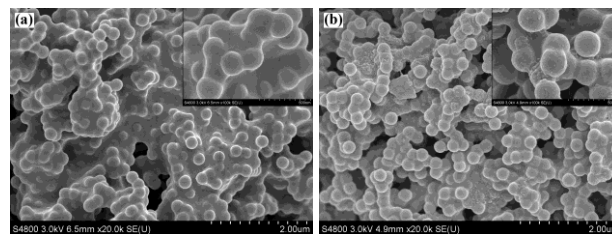


**Fig. 7** SEM images of S-15 coatings after (a) 4 cycles healing at ambient temperature; (b) 3 cycles healing followed by heat treatment

Recovering of superhydrophobicity of the etched coatings under ambient conditions is possible, however it takes time due to the limited movement of cured PDMS. Therefore, heating assisted healing of the plasma damaged coatings was also investigated. It was found that heat treatment shortened the time for healing of the superhydrophobicity, but speeded up the loss of PDMS at the surface. After 2 cycles of heat assisted healing, the plasma etched coating (S-15) did not become superhydrophobic, as shown in Fig. 8. However, THF treatment could further turn the coating superhydrophobic (dash line in Fig. 8c). SEM images in Fig. 7(b) showed that heating of the coating had little effect on the morphology of the surfaces. The heat healing cycles became longer with longer spray times (from S-5 sample to S-20 in Fig. 8), which also might be due to the limited rotation of PDMS chains in a thin spray coating.

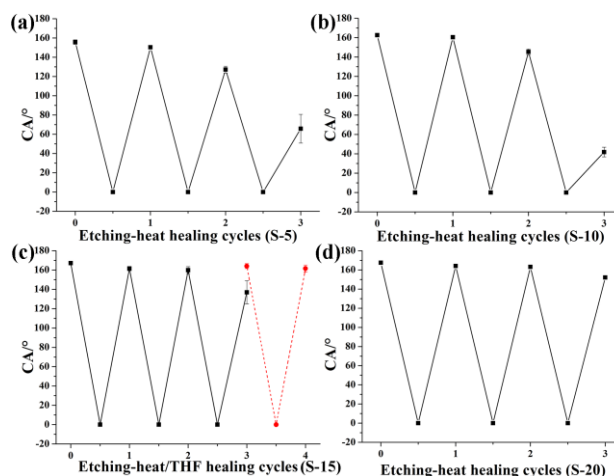


**Fig. 8** Self-healing cycles of coating healed by heat (solid line) first and then healed by THF swelling/curing (dash line): (a) S-5, (b) S-10, (c) S-15, and (d) S-20.

As mentioned previously, THF could help migration of PS toward the outer surface of the PS/SiO<sub>2</sub> particles and lower the surface energy. Therefore, heating and THF treatment could be used in combination to heal the superhydrophobic coatings. After THF swelling and heat treatment, PDMS between particles and PS in the core of particles could be driven to the surface and heal the coating, returning it to a superhydrophobic one. It was found that using the THF/heat healing process could repair the coating for more than 5 cycles, as shown in Fig. 9. The self-healing cycles become shorter with longer spray times. From the SEM images in Fig. 10(a), the S-5 surface showed a lot of polymer covering after 9 cycles THF healing, which might be PDMS and PS, resulting in it remaining superhydrophobic. In contrast, other surfaces had less PS and PDMS due to the THF spraying that rinsed polymers into spaces between the particles and emptied many particles with

holes formed in the shells, as shown in the inset of Fig. 10(b). This resulted in hydrophilic surfaces.

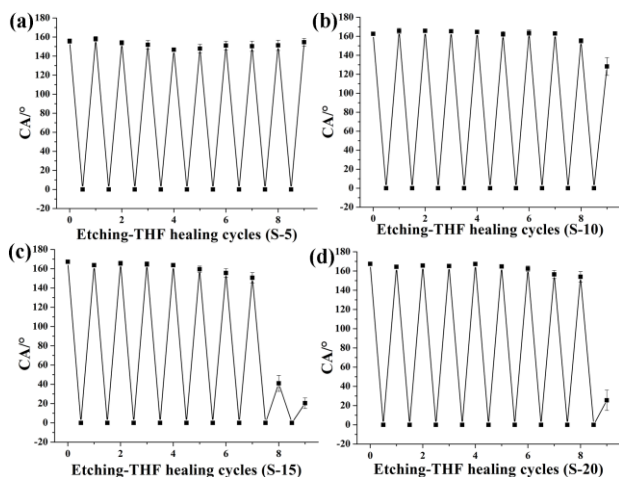


**Fig. 9** Self-healing cycles of coatings healed by THF: (a) S-5, (b) S-10, (c) S-15, and (d) S-20.

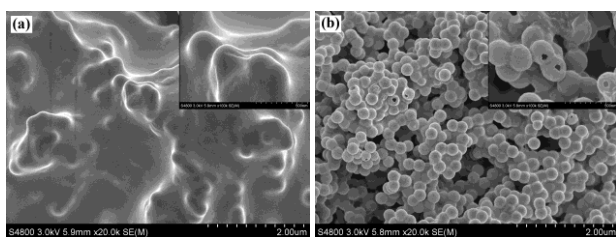


**Fig. 10** SEM images of coatings after 9 cycles THF healing: (a) S-5, (b) S-15.

Fig. 11 displays the X-ray photoelectron spectra of the as-prepared superhydrophobic S-15 coating (a), plasma etched coating (b), and THF (with spraying time of 4 s) healed coating (c). The oxygen signal from the coating remarkably increased after air plasma etching and decreased after THF healing. The increase in O content was due to oxygen-containing hydrophilic groups and the decomposition of PDMS after air plasma etching, which led to the coating becoming superhydrophilic. Also, PS and PDMS could be released to the surface after THF swelling and heat curing, leading to a decrease in O content and rendering the coating superhydrophobic.

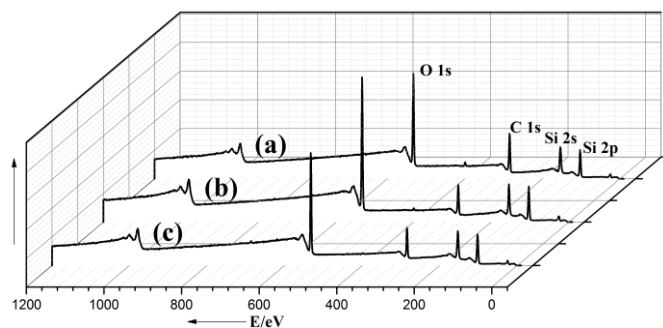


**Fig. 11** XPS of S-15 samples of (a) original superhydrophobic coating, (b) the same coating after air plasma etching for 5 min, and (c) the coating healed by THF and heat.

## Conclusions

Superhydrophobic surfaces were successfully fabricated by coating of polystyrene/SiO<sub>2</sub> core/shell nanoparticles and PDMS.

The surfaces showed lasting superhydrophobicity as demonstrated by cycles of sand abrasion. The resultant coatings could automatically and repeatedly heal their superhydrophobicity after damage at ambient temperature or by THF treatment and heating, which utilized the migration and movement of PDMS and PS in the core of particles. These self-healing superhydrophobic coatings are anticipated to have important practical applications because of their lasting and self-healing ability, and convenient use in outdoor coatings.

## Acknowledgements

This work was supported by National Natural Science Foundation of China (51372146), Program for New Century Excellent Talents in University (NCET-12-1042), Research Fund for the Doctoral Program of Higher Education of China (20116125110002, 20136125110003), Major Program of Science Foundation of Shaanxi Province (2011ZKC05-7), and Key Scientific Research Group of Shaanxi Province (2013KCT-08).

## Notes and references

- C.-H. Xue and J.-Z. Ma, *Journal of Materials Chemistry A*, 2013, **1**, 4146-4161.
- C.-H. Xue, P. Zhang, J.-Z. Ma, P.-T. Ji, Y.-R. Li and S.-T. Jia, *Chemical Communications*, 2013, **49**, 3588-3590.
- H. Zhou, H. Wang, H. Niu, A. Gestos, X. Wang and T. Lin, *Advanced Materials*, 2012, **24**, 2409-2412.
- C.-H. Xue, S.-T. Jia, J. Zhang and J.-Z. Ma, *Science and Technology of Advanced Materials*, 2010, **11**, 033002.
- J. Zimmermann, F. A. Reifler, G. Fortunato, L.-C. Gerhardt and S. Seeger, *Advanced Functional Materials*, 2008, **18**, 3662-3669.
- Z. Chu and S. Seeger, *Chemical Society Reviews*, 2014, **43**, 2784-2798.
- X.-M. Li, D. Reinhoudt and M. Crego-Calama, *Chemical Society Reviews*, 2007, **36**, 1350-1368.
- K. Liu, X. Yao and L. Jiang, *Chemical Society Reviews*, 2010, **39**, 3240-3255.
- L. Yao and J. He, *Progress in Materials Science*, 2014, **61**, 94-143.
- Y. Li, S. Chen, M. Wu and J. Sun, *Advanced Materials*, 2014, DOI: 10.1002/adma.201306136
- G. R. J. Artus and S. Seeger, *Industrial & Engineering Chemistry Research*, 2012, **51**, 2631-2636.
- E. Ueda and P. A. Levkin, *Advanced Materials*, 2013, **25**, 1234-1247.
- T. Verho, C. Bower, P. Andrew, S. Franssila, O. Ikkala and R. H. A. Ras, *Advanced Materials*, 2011, **23**, 673-678.
- L. Ionov and A. Synytska, *Physical Chemistry Chemical Physics*, 2012, **14**, 10497-10502.
- E. Huovinen, L. Takkunen, T. Korpela, M. Suvanto, T. T. Pakkanen and T. A. Pakkanen, *Langmuir*, 2014, **30**, 1435-1443.
- V. Kondrashov and J. Riise, *Langmuir*, 2014, **30**, 4342-4350.
- C. Su, Y. Xu, F. Gong, F. Wang and C. Li, *Soft Matter*, 2010, **6**, 6068-6071.
- X. Deng, L. Mammen, H.-J. Butt and D. Vollmer, *Science*, 2012, **335**, 67-70.
- X. Deng, L. Mammen, Y. Zhao, P. Lellig, K. Müllen, C. Li, H.-J. Butt and D. Vollmer, *Advanced Materials*, 2011, **23**, 2962-2965.

20. H. Jin, X. Tian, O. Ikkala and R. H. A. Ras, *ACS Applied Materials & Interfaces*, 2013, **5**, 485-488.
21. A. C. C. Esteves, Y. Luo, M. W. P. van de Put, C. C. M. Carcouët and G. de With, *Advanced Functional Materials*, 2013, **24**, 986-992.
22. X. Wang, X. Liu, F. Zhou and W. Liu, *Chemical Communications*, 2011, **47**, 2324-2326.
23. Q. Liu, X. Wang, B. Yu, F. Zhou and Q. Xue, *Langmuir*, 2012, **28**, 5845-5849.
24. T. Dikić, W. Ming, R. A. T. M. van Benthem, A. C. C. Esteves and G. de With, *Advanced Materials*, 2012, **24**, 3701-3704.
25. U. Manna and D. M. Lynn, *Advanced Materials*, 2013, **25**, 5104-5108.
26. Q. Wang, J. Li, C. Zhang, X. Qu, J. Liu and Z. Yang, *Journal of Materials Chemistry*, 2010, **20**, 3211-3215.
27. Y. Li, L. Li and J. Sun, *Angewandte Chemie*, 2010, **122**, 6265-6269.
28. H. Wang, Y. Xue, J. Ding, L. Feng, X. Wang and T. Lin, *Angewandte Chemie International Edition*, 2011, **50**, 11433-11436.
29. H. Wang, H. Zhou, A. Gestos, J. Fang and T. Lin, *ACS Applied Materials & Interfaces*, 2013, **5**, 10221-10226.
30. J. Hu, M. Chen, X. Fang and L. Wu, *Chemical Society Reviews*, 2011, **40**, 5472-5491.
31. Y. Bao, Y. Yang and J. Ma, *Journal of Colloid and Interface Science*, 2013, **407**, 155-163.
32. R.-k. Wang, H.-r. Liu and F.-w. Wang, *Langmuir*, 2013, **29**, 11440-11448.
33. A. I. Neto, H. J. Meredith, C. L. Jenkins, J. J. Wilker and J. F. Mano, *RSC Advances*, 2013, **3**, 9352-9356.
34. X. Li, C. Wang, Y. Yang, X. Wang, M. Zhu and B. S. Hsiao, *ACS Applied Materials & Interfaces*, 2014, **6**, 2423-2430.
35. X. Zhang, X. Yao, X. Wang, L. Feng, J. Qu and P. Liu, *Soft Matter*, 2014, **10**, 873-881.
36. D. S. Facio and M. J. Mosquera, *ACS Applied Materials & Interfaces*, 2013, **5**, 7517-7526.